Influenza A (H1N1) pneumonia: HRCT findings*

Pneumonia por vírus influenza A (H1N1): aspectos na TCAR

Viviane Brandão Amorim, Rosana Souza Rodrigues, Miriam Menna Barreto, Gláucia Zanetti, Bruno Hochhegger, Edson Marchiori

Abstract

Objective: To describe aspects found on HRCT scans of the chest in patients infected with the influenza A (H1N1) virus. **Methods:** We retrospectively analyzed the HRCT scans of 71 patients (38 females and 33 males) with H1N1 infection, confirmed through laboratory tests, between July and September of 2009. The HRCT scans were interpreted by two thoracic radiologists independently, and in case of disagreement, the decisions were made by consensus. **Results:** The most common HRCT findings were ground-glass opacities (85%), consolidation (64%), or a combination of ground-glass opacities and consolidation (58%). Other findings were airspace nodules (25%), bronchial wall thickening (25%), interlobular septal thickening (21%), crazy-paving pattern (15%), perilobular pattern (3%), and air trapping (3%). The findings were frequently bilateral (89%), with a random distribution (68%). Pleural effusion, when observed, was typically minimal. No lymphadenopathy was identified. **Conclusions:** The most common findings were ground-glass opacities and consolidations, or a combination of both. Involvement was commonly bilateral with no axial or craniocaudal predominance in the distribution. Although the major tomographic findings in H1N1 infection are nonspecific, it is important to recognize such findings in order to include infection with the H1N1 virus in the differential diagnosis of respiratory symptoms.

Keywords: Pneumonia, viral; Tomography, X-ray computed; Influenza A virus, H1N1 subtype.

Resumo

Objetivo: Descrever os aspectos encontrados em TCAR do tórax de pacientes infectados pelo vírus influenza A (H1N1). **Métodos:** Foram analisadas retrospectivamente as TCAR de 71 pacientes (38 femininos e 33 masculinos) com diagnóstico confirmado de influenza A (H1N1) através da identificação laboratorial do vírus, estudados no período entre julho e setembro de 2009. A interpretação das TCAR foi realizada por dois radiologistas torácicos de forma independente, e, em caso de discordância, as decisões foram tomadas por consenso. **Resultados:** Os achados de TCAR mais comuns foram opacidades em vidro fosco (85%), consolidação (64%) ou a combinação de opacidades em vidro fosco e consolidação (58%). Outros achados foram nódulos do espaço aéreo (25%), espessamento das paredes brônquicas (25%), espessamento de septos interlobulares (21%), padrão de pavimentação em mosaico (15%), espessamento perilobular (3%) e aprisionamento aéreo (3%). As alterações foram frequentemente bilaterais (89%), com distribuição não específica (68%). Derrame pleural, quando observado, foi, em geral, de pequena monta. Não foram observadas linfonodomegalias. **Conclusões:** As alterações predominantes foram opacidades em vidro fosco, consolidações ou a combinação de ambas. O acometimento foi frequentemente bilateral e não houve predomínio quanto à distribuição (axial ou craniocaudal). Apesar de inespecíficos, é importante reconhecer os principais aspectos tomográficos da infecção por influenza A (H1N1) a fim de incluir essa possibilidade no diagnóstico diferencial de sintomas respiratórios.

Descritores: Pneumonia viral; Tomografia computadorizada por raios X; Vírus da influenza A subtipo H1N1.

---

* Study carried out at the Federal University of Rio de Janeiro, Rio de Janeiro, Brazil.
Correspondence to: Edson Marchiori. Rua Thomaz Cameron, 438, Valparaiso, CEP 25685-120, Petrópolis, RJ, Brasil.
Tel. 55 24 2249-2777. Fax: 55 21 2629-9017. E-mail: edmarchiori@gmail.com
Financial support: None.
Submitted: 22 January 2013. Accepted, after review: 4 March 2013.

Introduction

In April of 2009, there began an epidemic of acute febrile respiratory illness caused by a new virus: the influenza A (H1N1) virus. The first cases occurred in Mexico, and the infection rapidly spread worldwide.[1] By August of 2010, 214 countries had been hit by the infection and more than 18,000 deaths had been confirmed.[1,2]

Although the number of cases of H1N1 infection has decreased significantly since the 2009 pandemic, various studies have reported that the virus is still circulating together with other seasonal viruses, with different prevalences. In Brazil, by October of 2012, approximately 20,000 patients had been hospitalized for severe acute respiratory syndrome. Of those, approximately 2,600 cases were caused by the influenza A (H1N1) post-pandemic virus.[3]

The most common clinical findings in the presentation of H1N1 infection are fever, cough, dyspnea, myalgia, and headache. Gastrointestinal symptoms, such as nausea, vomiting, and diarrhea, have also been reported.[4-6] In most cases, the symptoms are mild and run a self-limiting course; however, a small proportion of individuals develop a severe course, which can result in respiratory failure and death.[4,7-10]

The most common laboratory test findings include increased serum lactate dehydrogenase levels (which can exceed 1,000 IU/L), bearing in mind that elevated lactate dehydrogenase levels are significantly associated with disease severity and ICU admission[6,11]; increased C-reactive protein levels; increased serum creatine kinase levels; lymphopenia; and thrombocytopenia. Elevated transaminase and D-dimer levels can occur in some patients.[4,7,12]

Chest X-ray provides adequate information for defining the approach in most of the affected patients.[13] However, HRCT often becomes an important tool for determining the extent of pulmonary involvement, as well as being useful in the evaluation of complications and in the clarification of suspected mixed infections or failure to respond to therapy.[4] Although the diagnosis of viral infection is based on the clinical profile and on identification of the virus, the recognition of some imaging features of the disease can become useful, especially in patients with *forme fruste* or atypical clinical manifestations. Therefore, the understanding of the imaging features of the disease becomes important in clinical practice.

The objective of the present study was to evaluate, by means of a retrospective analysis of HRCT scans of patients with confirmed H1N1 infection, the most common tomographic findings and the characteristics of their distribution in the lung parenchyma.

Methods

The study was approved by the Research Ethics Committee of the Clementino Fraga Filho University Hospital. This was a retrospective observational cross-sectional study in which we analyzed the HRCT scans of 71 patients from several hospitals in different states in Brazil between July and September of 2009.

The study population included patients presenting with flu-like symptoms and diagnosed with H1N1 infection, regardless of age or gender. The inclusion criterion was the diagnostic confirmation of H1N1 infection through laboratory testing (viral culture or real-time PCR) of aspiration material or of nasopharyngeal or oropharyngeal swab specimens. Another inclusion criterion was the required availability of complete chest HRCT scans of each study patient, performed during the acute phase of the disease. Patients with other pulmonary infections, confirmed through laboratory tests, were excluded, as were those with tomographic findings suggestive of pulmonary involvement resulting from chronic lung diseases. All HRCT scans were obtained 2-10 days after the onset of symptoms.

As multiple institutions were involved, imaging examination was performed with different tomography scanners, using the high-resolution technique, in accordance with the following protocol: patient in the supine position; 1- to 2-mm slice thickness in increments of up to 10 mm, from the lung apices through the hemidiaphragm, at the end of a deep inhalation; and a high spatial resolution reconstruction algorithm. Parenchymal and mediastinal window settings (width = 1,400-1,600 HU; level = −600 to −800 HU; and width = 350-450 HU; level = 15-25 HU, respectively) were used.

The following tomographic characteristics were analyzed: pattern of the findings (airspace consolidations, ground-glass opacities, airspace nodules, interlobular septal thickening, crazy-paving pattern, air trapping—when identified in

the inspiratory phase—and peribronchovascular interstitial thickening); and distribution of the lesions (central, peripheral, or random; unilateral or bilateral; upper, middle, or lower lung zone predominant, or any combination of the three). In addition, the presence of pleural effusion and lymphadenopathy was evaluated. The HRCT scans were independently interpreted by two experienced thoracic radiologists, and in case of disagreement, the decisions were made by consensus.

Consolidation was defined as increased attenuation of the lung parenchyma, resulting in the obscuration of the vascular outlines and adjacent airway walls; ground-glass opacity was defined as slightly increased attenuation of the lung parenchyma that is unrelated to the obscuration of the vessels and adjacent airway walls; interlobular septal thickening was defined as thin linear opacities, which correspond to the thickened peripheral connective septa; a crazy-paving pattern was defined as interlobular septal thickening superimposed on ground-glass opacities; airspace nodules were defined as ill-defined nodules smaller than 1 cm and tending to confluence; peribronchovascular thickening was defined as an increase in connective tissue around the bronchi, pulmonary arteries, and lymphatic vessels; a perilobular pattern was defined as thick and irregular polygonal opacities in the periphery of the secondary pulmonary lobule; and air trapping was defined as decreased attenuation of the lung parenchyma, revealed by a lower-than-usual density.[14,15] The bronchial walls were considered thickened if the bronchial lumen internal diameter was equal to or greater than 80% of its external diameter.[16]

The distribution of the lesions in the lung parenchyma was evaluated along the axial and craniocaudal axes. The craniocaudal distribution of the lesions was classified as upper, middle, or lower lung zone predominant, or any combination of the three. The axial distribution of the findings was classified as central or peripheral. In addition, the predominance of the findings in one lung or the lack of predominance along the two axes was recorded.

Results

Of the 71 patients, 38 (53.53%) and 33 (46.47%) were female and male, respectively. The mean age of the patients was 41.3 years (range, 16-92 years).

Pulmonary abnormalities were identified on the HRCT scans of all patients. The most common tomographic findings, in decreasing order, were as follows: ground-glass opacities, in 60 patients (85%); consolidations, in 46 (64%; Figures 1 and 2); airspace nodules, in 18 (25%; Figure 3); bronchial wall thickening, in 18 (25%); interlobular septal thickening, with or without ground-glass opacities, in 15 (21%); crazy-paving pattern, in 11 (15%); perilobular pattern, in 2 (3%); and air trapping, 2 (3%; Figure 4 and Table 1).

The most common findings were ground-glass opacities and consolidations. A combination of ground-glass opacities and consolidations in the same patient was observed in 41 cases (58%). Only 6 patients had no ground-glass opacities, consolidations, or a combination of both.

Of the patients who had ground-glass opacities, 11 (15%) also had interlobular septal thickening, characterizing a crazy-paving pattern. Septal thickening, without ground-glass opacities, was a mild secondary finding in 4 patients (6%). Airspace nodules were found in 18 cases (25%), and bronchial wall thickening was found in 18 (25%). Bronchial wall thickening was observed in all 6 patients who had no ground-glass opacities, consolidations, or a combination of both.

Air trapping was an uncommon finding, being observed in 2 patients. Peribronchovascular interstitial thickening was observed in 8 cases (11%), and, in all of these cases, there were ground-glass opacities and consolidations. A perilobular pattern was found in only 2 patients (3%). Minimal pleural effusion was observed in 19 patients (27%), being bilateral in 10 (52%).

Parenchymal involvement was bilateral in 63 cases (89%) and unilateral in 8 (11%). In 55 patients (77%), the lesions were evenly distributed between the two lungs; in 9 patients (13%), the lesions predominantly affected the right lung; and, in 7 patients (10%), the lesions predominantly affected the left lung. In 7 of the 8 cases (87%) in which the involvement was unilateral, only one lobe was affected. An analysis of the craniocaudal distribution of the lesions by lung zone revealed the following: no preferential distribution, in 35 patients (49%); lower third predominance, in 26 (37%); middle third predominance, in 4 (6%); lower and middle third predominance, in 5 (7%); and upper third

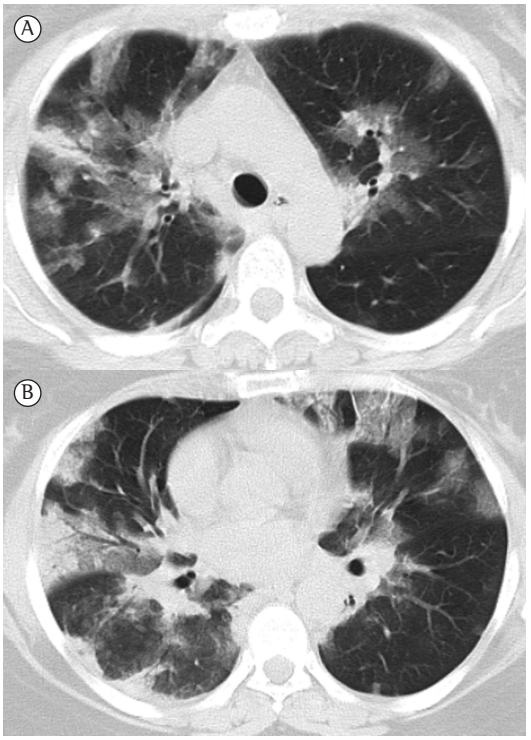

Figure 1 - HRCT scans. In A, areas of consolidation and ground-glass opacities in the upper lobes of both lungs. In B, areas of consolidation and ground-glass opacities in the lower lobes, with peripheral distribution of the lesions.

predominance, in only 1 (1.5%). An analysis of the axial distribution of the lesions revealed the following: no specific distribution, in 48 patients (68%); peripheral lung zone predominance, in 21 (29%); and central lung zone predominance, in 2 (3%). In 14 of the 21 patients (67%) with peripheral distribution, there were also lesions in the peribronchovascular interstitial space.

Discussion

In the present study, we retrospectively evaluated the HRCT scans of 71 patients with confirmed H1N1 infection. The most common tomographic findings were ground-glass opacities, consolidations, and a combination of ground-glass opacities and consolidations in the same patient. These data are similar to literature data showing that these tomographic findings predominate in patients with H1N1 infection.[4,17-21]

A crazy-paving pattern, in which ground-glass opacities are associated with septal thickening, has been reported in few cases in the literature.[22,23] In our study, 15% of the patients showed

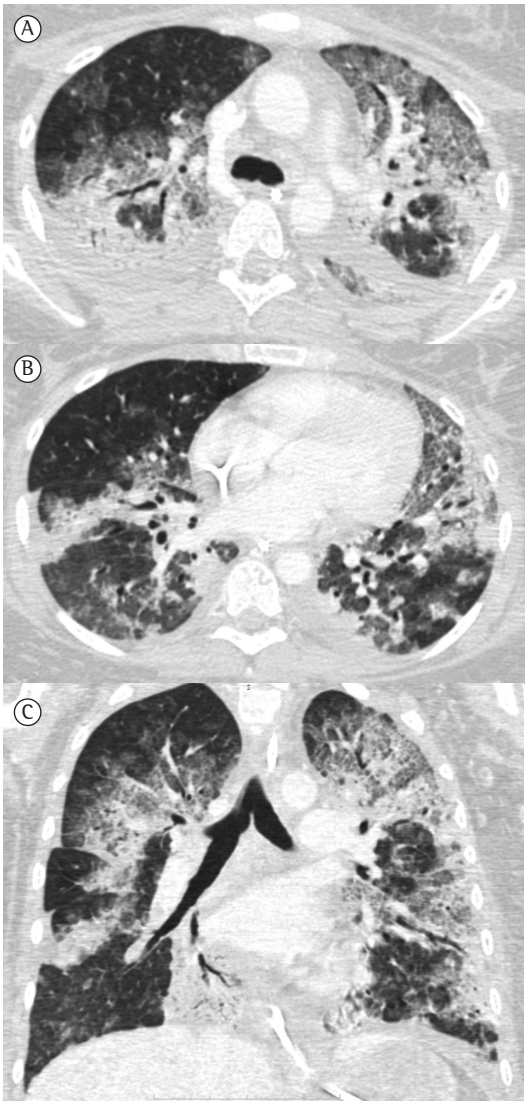

Figure 2 - Axial HRCT slices at the levels of the upper lobes (A) and lower lobes (B), as well as reformatted coronal image (C), showing extensive areas of consolidation with air bronchograms in both lungs.

this pattern. Septal thickening without ground-glass opacities was a mild secondary finding, being observed in only 4 patients (6%).

Airspace nodules were present in 25% of the cases, and this was the dominant finding in only 1. This finding has not commonly been reported in the literature, and few studies have described the presence of airspace nodules in patients with H1N1 infection.[21,24] This can be attributed to an alternative interpretation, by some authors, of airspace nodules being focal areas of consolidation, or it can even be attributed to the fact that airspace nodules can be obscured by

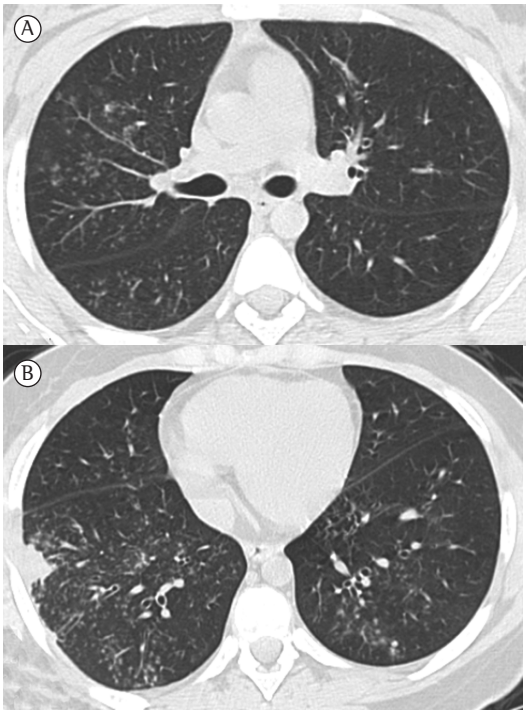

Figure 3 - Axial HRCT slices at the levels of the upper lobes (A) and lower lobes (B) revealing multiple small centrilobular nodules, some of which have a tree-in-bud pattern, distributed principally in the middle lobe and lower lobes. Note also bronchial wall thickening predominantly in the right lower lobe, as well as a small area of peripheral consolidation.

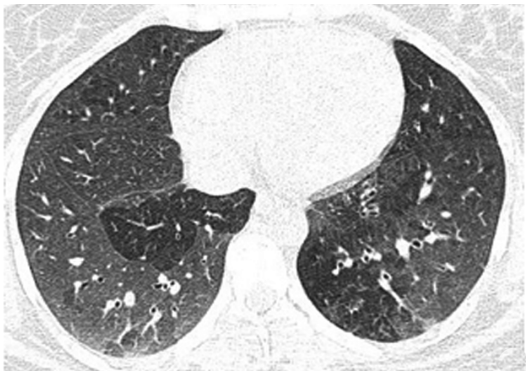

Figure 4 - Axial HRCT slice at the level of the lower lobes, obtained during the expiratory phase, showing bilateral areas of mosaic attenuation, as well as a well-defined area of air trapping in the lower lobe of the left lung.

other findings when there is extensive involvement by the disease.

Bronchial wall thickening was observed in one fourth of the patients in our sample. In the literature, these findings have been described in few studies and in varying frequencies.[21,24] One group of authors[24] found bronchial wall thickening in all of their patients. Other authors[25] suggested that these changes occur early in the disease course, a period when patients have not yet sought medical care, and is therefore poorly reported. Tanaka et al.[25] related the high frequency of these findings in their study (68%) to the fact that their patients had quick access to medical treatment. Likewise, the immunocompromised patients in another study[24] are probably patients who received prompt medical attention, given their comorbidities. In contrast, other authors[20] reported air trapping in a female patient in a late phase, three months after the onset of the disease.

Table 1 - Frequency distribution of the tomographic findings in the 71 patients in the sample.

Finding	Frequency	
	n	%
Ground-glass opacities	60	85
Consolidations	46	64
Airspace nodules	18	25
Bronchial wall thickening	18	25
Interlobular septal thickening	15	21
Crazy-paving pattern	11	15
Perilobular pattern	2	3
Air trapping	2	3

In our sample, a mosaic attenuation pattern was observed in 3% of the cases and was interpreted as being air trapping because it was associated with bronchial wall thickening. As occurred in our sample, air trapping related to H1N1 infection has rarely been described in the literature.[21,24] However, it should be emphasized that, in those studies, the expiratory phase, which increases sensitivity in the characterization of this pattern, was not performed. Li et al.[21] found a mosaic attenuation pattern due to air trapping in 13% of their patients and related it to the use of mechanical ventilation.

A perilobular pattern is a finding that is commonly associated with organizing pneumonia.[15] This finding was seen in 2 of our patients (3%), and it had not been described in H1N1 infection. Because patients affected by the pandemic virus can develop organizing pneumonia during the convalescence phase of the disease,[18,19,26] a perilobular pattern is an expected finding in these cases.

In the literature, the most common distribution of HRCT findings is bilateral multifocal involvement predominantly in the lower lobes.[4,20,21,24] However, in some studies, the distribution is diffuse, with no zonal predominance.[27] In our sample, the HRCT scans showed bilateral involvement in the vast majority of the cases (89%), and both lungs were similarly affected in 77% of them. The craniocaudal distribution of the lesions was random, with no zonal predominance in approximately half of the cases and with lower third predominance in 37%. The axial distribution of the findings showed no zonal predominance in most cases (68%), but, in approximately one third of the cases, it showed peripheral lung zone predominance. A central distribution was rarely observed. In the literature, data regarding the axial distribution of HRCT findings are varied, there being reports of central or peripheral predominance.[4,20,24] Regarding the craniocaudal distribution, the literature reports lower lung zone predominance.

Pleural effusion, either unilateral or bilateral and typically minimal, has been described in some cases.[4,17,21] In our sample, pleural effusion was observed in 27% of the cases, being bilateral in 52% and typically minimal. No mediastinal lymphadenopathy was identified in any of the patients studied.

Our study had some limitations. First, the study was retrospective, which made it impossible to establish a proper correlation between clinical and radiological findings. Second, there were some differences in relation to the technical parameters in tomography image acquisition, since we evaluated HRCT scans performed at various institutions.

In conclusion, the most common tomographic findings were ground-glass opacities and airspace consolidations, or a combination of both. The findings were predominantly bilateral, with no axial or craniocaudal predominance in the distribution in most cases. When zonal predominance was present, it was more common in the lower thirds and peripheral regions of the lungs. Pleural effusion, when observed, was typically minimal. No lymphadenopathy was identified. Although the major tomographic findings in H1N1 infection are nonspecific, it is important to recognize such findings in order to include infection with the H1N1 virus in the differential diagnosis of respiratory symptoms

References

1. World Health Organization [homepage on the Internet]. Geneva: World Health Organization [cited 2012 Dec 21]. Pandemic Influenza A (H1N1). [Adobe Acrobat document, 72p.]. Available from: http://www.who.int/csr/resources/publications/swineflu/h1n1_donor_032011.pdf
2. Cao B, Li XW, Mao Y, Wang J, Lu HZ, Chen YS, et al. Clinical features of the initial cases of 2009 pandemic influenza A (H1N1) virus infection in China. N Engl J Med. 2009;361(26):2507-17. http://dx.doi.org/10.1056/NEJMoa0906612 PMid:20007555
3. Portal da Saúde [homepage on the Internet]. Brasília: Ministério da Saúde [updated 2012 Nov 7; cited 2012 Nov 14]. Boletim Informativo - Secretaria de Vigilância em Saúde - Influenza (gripe) - Semana Epidemiológica (SE) 44. Available from: http://portalsaude.saude.gov.br/portalsaude/noticia/8100/785/boletim-informativo-de-influenza:-semana-epidemiologica-44.html.
4. Marchiori E, Zanetti G, Hochhegger B, Rodrigues RS, Fontes CA, Nobre LF, et al. High-resolution computed tomography findings from adult patients with Influenza A (H1N1) virus-associated pneumonia. Eur J Radiol. 2010;74(1):93-8. Erratum in: Eur J Radiol. 2011;80(2):623. Meirelles, Gustavo [corrected to Meirelles, Gustavo Souza Portes]. http://dx.doi.org/10.1016/j.ejrad.2009.11.005 PMid:19962842
5. Lenzi L, Mello ÂM, Silva LR, Grochocki MH, Pontarolo R. Pandemic influenza A (H1N1) 2009: risk factors for hospitalization. J Bras Pneumol. 2012;38(1):57-65. http://dx.doi.org/10.1590/S1806-37132012000100009 PMid:22407041
6. Nicolini A, Claudio S, Rao F, Ferrera L, Isetta M, Bonfiglio M. Influenza A (H1N1)-associated pneumonia. J Bras Pneumol. 2011;37(5):621-7. PMid:22042394
7. Perez-Padilla R, de la Rosa-Zamboni D, Ponce de Leon S, Hernandez M, Qui-ones-Falconi F, Bautista E, et al. Pneumonia and respiratory failure from swine-origin influenza A (H1N1) in Mexico. N Engl J Med. 2009;361(7):680-9. http://dx.doi.org/10.1056/NEJMoa0904252 PMid:19564631
8. Marchiori E, Zanetti G, D'Ippolito G, Verrastro CG, Meirelles GS, Capobianco J, et al. Swine-origin influenza A (H1N1) viral infection: thoracic findings on CT. AJR Am J Roentgenol. 2011;196(6):W723-8. http://dx.doi.org/10.2214/AJR.10.5109 PMid:21606260
9. Asai N, Ohkuni Y, Kaneko N, Kawamura Y, Aoshima M. A successfully treated case of parainfluenza virus 3 pneumonia mimicking influenza pneumonia. J Bras Pneumol. 2012;38(6):810-2. http://dx.doi.org/10.1590/S1806-37132012000600020 PMid:23288130
10. Mauad T, Hajjar LA, Callegari GD, da Silva LF, Schout D, Galas FR, et al. Lung pathology in fatal novel human influenza A (H1N1) infection. Am J Respir Crit Care Med. 2010;181(1):72-9. http://dx.doi.org/10.1164/rccm.200909-1420OC PMid:19875682
11. Cui W, Zhao H, Lu X, Wen Y, Zhou Y, Deng B, et al. Factors associated with death in hospitalized pneumonia patients with 2009 H1N1 influenza in Shenyang, China. BMC Infect Dis. 2010;10:145. http://dx.doi.org/10.1186/1471-2334-10-145 PMid:20513239 PMCid:2890005
12. Marchiori E, Zanetti G, Hochhegger B, Mauro Mano C. High-resolution CT findings in a patient with influenza A (H1N1) virus-associated pneumonia. Br J

Radiol. 2010;83(985):85-6. http://dx.doi.org/10.1259/bjr/26459688 PMid:20139251 PMCid:3487267
13. Aviram G, Bar-Shai A, Sosna J, Rogowski O, Rosen G, Weinstein I, et al. H1N1 influenza: initial chest radiographic findings in helping predict patient outcome. Radiology. 2010;255(1):252-9. http://dx.doi.org/10.1148/radiol.10092240 PMid:20308461
14. Hansell DM, Bankier AA, MacMahon H, McLoud TC, Müller NL, Remy J. Fleischner Society: glossary of terms for thoracic imaging. Radiology. 2008;246(3):697-722. http://dx.doi.org/10.1148/radiol.2462070712 PMid:18195376
15. Silva CI, Marchiori E, Souza Júnior AS, Müller NL; Comissão de Imagem da Sociedade Brasileira de Pneumologia e Tisiologia. Illustrated Brazilian consensus of terms and fundamental patterns in chest CT scans. J Bras Pneumol. 2010;36(1):99-123. http://dx.doi.org/10.1590/S1806-37132010000100016 PMid:20209314
16. Muller NL, Silva IC. Bronchial abnormalities. In: Muller NL, Silva IS, editors. High-yield imaging. Chest. Philadelphia: Saunders/Elsevier; 2010. p. 438-47.
17. Li P, Zhang JF, Xia XD, Su DJ, Liu BL, Zhao DL, et al. Serial evaluation of high-resolution CT findings in patients with pneumonia in novel swine-origin influenza A (H1N1) virus infection. Br J Radiol. 2012;85(1014):729-35. http://dx.doi.org/10.1259/bjr/85580974 PMid:22167502
18. Marchiori E, Zanetti G, Fontes CA, Santos ML, Valiante PM, Mano CM, et al. Influenza A (H1N1) virus-associated pneumonia: high-resolution computed tomography-pathologic correlation. Eur J Radiol. 2011;80(3):e500-4. http://dx.doi.org/10.1016/j.ejrad.2010.10.003 PMid:21035974
19. Marchiori E, Zanetti G, Mano CM, Hochhegger B, Irion KL. Follow-up aspects of influenza A (H1N1) virus-associated pneumonia: the role of high-resolution computed tomography in the evaluation of the recovery phase. Korean J Radiol. 2010;11(5):587. http://dx.doi.org/10.3348/kjr.2010.11.5.587 PMid:20808707 PMCid:2930172
20. Marchiori E, Zanetti G, Mano CM. Swine-origin influenza A (H1N1) viral infection: small airways disease. AJR Am J Roentgenol. 2010;195(4):W317; author reply W318.
21. Rodrigues RS, Marchiori E, Bozza FA, Pitrowsky MT, Velasco E, Soares M, et al. Chest computed tomography findings in severe influenza pneumonia occurring in neutropenic cancer patients. Clinics (Sao Paulo). 2012;67(4):313-8. http://dx.doi.org/10.6061/clinics/2012(04)03
22. Marchiori E, Zanetti G, D'Ippolito G, Hochhegger B. Crazy-paving pattern on HRCT of patients with H1N1 pneumonia. Eur J Radiol. 2011;80(2):573-5. http://dx.doi.org/10.1016/j.ejrad.2010.10.004 PMid:21035973
23. Henzler T, Meyer M, Kalenka A, Alb M, Schmid-Bindert G, Bartling S, et al. Image findings of patients with H1N1 virus pneumonia and acute respiratory failure. Acad Radiol. 2010;17(6):681-5. http://dx.doi.org/10.1016/j.acra.2010.03.013 PMid:20457412
24. Elicker BM, Schwartz BS, Liu C, Chen EC, Miller SA, Chiu CY, et al. Thoracic CT findings of novel influenza A (H1N1) infection in immunocompromised patients. Emerg Radiol. 2010;17(4):299-307. http://dx.doi.org/10.1007/s10140-010-0859-x PMid:20111882 PMCid:2880241
25. Tanaka N, Emoto T, Suda H, Kunihiro Y, Matsunaga N, Hasegawa S, et al. High-resolution computed tomography findings of influenza virus pneumonia: a comparative study between seasonal and novel (H1N1) influenza virus pneumonia. Jpn J Radiol. 2012;30(2):154-61. http://dx.doi.org/10.1007/s11604-011-0027-6 PMid:22180185
26. Marchiori E, Hochhegger B, Zanetti G. Organising pneumonia as a late abnormality in influenza A (H1N1) virus infection. Br J Radiol. 2012;85(1014):841; author reply 842. http://dx.doi.org/10.1259/bjr/91363092 PMid:22665929
27. Toufen C Jr, Costa EL, Hirota AS, Li HY, Amato MB, Carvalho CR. Follow-up after acute respiratory distress syndrome caused by influenza a (H1N1) virus infection. Clinics (Sao Paulo). 2011;66(6):933-7. http://dx.doi.org/10.1590/S1807-59322011000600002 PMCid:3129942

About the authors

Viviane Brandão Amorim
Master's Student in Radiology. Federal University of Rio de Janeiro, Rio de Janeiro, Brazil.

Rosana Souza Rodrigues
Radiologist. Federal University of Rio de Janeiro and D'Or Institute for Research and Education, Rio de Janeiro, Brazil.

Miriam Menna Barreto
Radiologist. Federal University of Rio de Janeiro, Rio de Janeiro, Brazil.

Gláucia Zanetti
Professor. Petrópolis School of Medicine, Petrópolis, Brazil.

Bruno Hochhegger
Radiologist. Santa Casa Hospital Complex in Porto Alegre, Porto Alegre, Brazil.

Edson Marchiori
Associate Professor of Radiology. Federal University of Rio de Janeiro, Rio de Janeiro, Brazil.